Frequent mutation of receptor protein tyrosine phosphatases provides a mechanism for STAT3 hyperactivation in head and neck cancer

Vivian Wai Yan Lui[a,1], Noah D. Peyser[a,b,1], Patrick Kwok-Shing Ng[c], Jozef Hritz[d,e], Yan Zeng[a], Yiling Lu[c], Hua Li[a], Lin Wang[a], Breean R. Gilbert[a], Ignacio J. General[f], Ivet Bahar[f], Zhenlin Ju[g], Zhenghe Wang[h], Kelsey P. Pendleton[a], Xiao Xiao[a], Yu Du[a], John K. Vries[f], Peter S. Hammerman[i], Levi A. Garraway[i], Gordon B. Mills[c], Daniel E. Johnson[b,j], and Jennifer R. Grandis[a,b,2]

Departments of [a]Otolaryngology, [b]Pharmacology and Chemical Biology, [d]Structural Biology, and [f]Computational and Systems Biology, University of Pittsburgh School of Medicine, Pittsburgh, PA 15213; [e]Central European Institute of Technology, Masaryk University, 625 00 Brno, Czech Republic; Departments of [c]Systems Biology and [g]Bioinformatics and Computational Biology, University of Texas MD Anderson Cancer Center, Houston, TX 77054; [h]Department of Genetics and Case Comprehensive Cancer Center, Case Western Reserve University, Cleveland, OH 44106; [i]Dana-Farber Cancer Institute, Harvard Medical School, Boston, MA 02215; and [j]Division of Hematology/Oncology, Department of Medicine, University of Pittsburgh Cancer Institute and University of Pittsburgh School of Medicine, Pittsburgh, PA 15213

Edited by George R. Stark, Lerner Research Institute, Cleveland Clinic Foundation, Cleveland, OH, and approved December 12, 2013 (received for review October 16, 2013)

The underpinnings of STAT3 hyperphosphorylation resulting in enhanced signaling and cancer progression are incompletely understood. Loss-of-function mutations of enzymes that dephosphorylate STAT3, such as receptor protein tyrosine phosphatases, which are encoded by the *PTPR* gene family, represent a plausible mechanism of STAT3 hyperactivation. We analyzed whole exome sequencing (n = 374) and reverse-phase protein array data (n = 212) from head and neck squamous cell carcinomas (HNSCCs). *PTPR* mutations are most common and are associated with significantly increased phospho-STAT3 expression in HNSCC tumors. Expression of receptor-like protein tyrosine phosphatase T (PTPRT) mutant proteins induces STAT3 phosphorylation and cell survival, consistent with a "driver" phenotype. Computational modeling reveals functional consequences of *PTPRT* mutations on phospho-tyrosine–substrate interactions. A high mutation rate (30%) of *PTPR*s was found in HNSCC and 14 other solid tumors, suggesting that *PTPR* alterations, in particular *PTPRT* mutations, may define a subset of patients where STAT3 pathway inhibitors hold particular promise as effective therapeutic agents.

STAT3 activation | driver mutations | phosphatase mutations

Tyrosine phosphorylation regulates a multitude of cellular processes by coordinately activating and inactivating signaling proteins. Aberrations of protein tyrosine phosphorylation and signaling are a hallmark for oncogenic events found in most human cancers. The phosphorylation/dephosphorylation of tyrosine residues on signaling proteins is directly mediated by protein tyrosine kinases and phosphatases. Although many cellular factors are known to dynamically control the activity of these enzymes, genetic alterations of kinases and phosphatases in human cancers lead to perturbations in the levels of tyrosine phosphorylated proteins, uncontrolled cell growth, and tumor formation. Although activating mutations of tyrosine kinases have been extensively studied (1, 2), cancer-associated mutations of tyrosine phosphatases remain incompletely understood, partly due to the lack of comprehensive genomic analysis of these large arrays of phosphatases, as well as their largely unknown and often ambiguous actions in normal physiology and cancer biology.

Among the 107 known protein tyrosine phosphatases, the receptor protein tyrosine phosphatases (RPTPs) represent the largest family of the human tyrosine phosphatome, comprising 21 family members (3). These RPTPs are believed to be crucial for the regulation of inter- as well as intracellular signaling due to the cell-surface localization of RPTPs. Selected members of the RPTP family have been reported to function as tumor suppressors, where gene mutation, deletion, or methylation may contribute to the cancer phenotype (3).

STAT3 is an oncogene, and constitutive STAT3 activation is a hallmark of human cancers. Activating STAT3 mutations are rare in all cancers studied to date, including head and neck squamous cell carcinoma (HNSCC) (4). Although activating mutations of upstream receptor tyrosine kinases leading to increased STAT3 phosphorylation characterize some malignancies [e.g., EGFR mutations in non-small cell lung cancer (5)], most cancers lack these alterations yet harbor elevated phospho-STAT3 (p-STAT3) levels. We (Z.W.) previously reported that STAT3 serves as a substrate for wild-type PTPRT enzyme (also known as RPTP-T, RPTPρ, or RPTPrho) in colorectal cancer cells (SW480 and HT29) and HEK293T cells (6). STAT3 has additionally been reported to be a substrate of PTPRD (also

Significance

Most cancers are characterized by increased STAT3 activation where phosphorylated STAT3 levels are associated with reduced survival. The molecular mechanisms underlying aberrant STAT3 phosphorylation/activation in human malignancies have been elusive. Our findings provide a mechanistic basis for tumor-specific STAT3 hyperactivation in head and neck squamous cell carcinoma (HNSCC). We demonstrate that receptor-like protein tyrosine phosphatases, encoded by *PTPR* genes, including *PTPRT*, are commonly mutated in HNSCC where *PTPR* mutations are associated with increased phosphorylation of STAT3 in tumors. Several cancer-related *PTPRT* mutations localize to the substrate interaction surface of the enzyme catalytic domains. Expression of mutated *PTPRT* in HNSCC models markedly increases STAT3 activation, promoting cellular survival. *PTPRT* mutations may therefore serve as predictive biomarkers for STAT3 pathway inhibitors, suggesting new therapeutic opportunities.

Author contributions: V.W.Y.L., N.D.P., P.K.-S.N., J.H., I.J.G., I.B., J.K.V., and J.R.G. designed research; V.W.Y.L., N.D.P., P.K.-S.N., J.H., Y.Z., Y.L., H.L., L.W., I.J.G., I.B., and X.X. performed research; V.W.Y.L., N.D.P., J.H., Y.L., and G.B.M. contributed new reagents/analytic tools; V.W.Y.L., N.D.P., P.K.-S.N., J.H., Y.L., B.R.G., I.J.G., I.B., Z.J., K.P.P., Y.D., P.S.H., G.B.M., and J.R.G. analyzed data; and V.W.Y.L., N.D.P., P.K.-S.N., J.H., I.J.G., Z.W., P.S.H., L.A.G., G.B.M., D.E.J., and J.R.G. wrote the paper.

Conflict of interest statement: J.R.G. receives research support from Bristol-Myers Squibb, Novartis, and Atellas (previously OSI Pharmaceuticals).

This article is a PNAS Direct Submission.

[1]V.W.Y.L. and N.D.P. contributed equally to this work.

[2]To whom correspondence should be addressed. E-mail: jgrandis@pitt.edu.

This article contains supporting information online at www.pnas.org/lookup/suppl/doi:10.1073/pnas.1319551111/-/DCSupplemental.

known as PTPδ) in glioblastoma models, suggesting that several RPTP family members may exhibit tumor-suppressive function by dephosphorylating STAT3 (7). In the present study, we hypothesized that mutation of RPTP family members, including *PTPRT,* results in elevated expression levels of tyrosine phosphorylated STAT3 in human HNSCC. Analysis of reverse-phase protein array and sequencing data demonstrated significant association between *PTPR* mutation and increased p-STAT3 expression levels in HNSCC, establishing the de novo signaling consequence of *PTPR* mutations on a major oncogenic pathway that drives human carcinogenesis. Studies in HNSCC models demonstrate that *PTPRT* mutations induce p-STAT3 and HNSCC survival, consistent with a "driver" phenotype whereas computational modeling revealed functional implications of *PTPR* mutations on phosphotyrosine (p-Tyr)–substrate interactions. Analysis of whole-exome sequencing results of 374 primary head and neck squamous cell carcinomas (HNSCCs) revealed that *PTPR* genes are mutated in nearly one-third (30.7%) of HNSCC tumors, compared with a 15.2% mutation rate in the cytoplasmic protein tyrosine phosphatase (PTP) family. This pattern is strikingly consistent across an additional 14 types of solid tumors sequenced to date, implicating a potentially important pathologic contribution of *PTPR* mutations to human carcinogenesis. These cumulative findings suggest that genetic alterations of selected *PTPRs*, including *PTPRT*, may induce STAT3 activation and serve as predictive biomarkers for treatment with emerging STAT3 pathway inhibitors.

Results

PTPR Mutations Significantly Correlate with in Situ p-STAT3(Y705) Up-Regulation in HNSCC Patient Tumors. To date, associations between *PTPR* alterations and human cancers have relied on cell-line models. It remains undetermined whether tumor-specific mutations of these key tyrosine phosphatases mediate STAT3 hyperactivation in human tumors, including HNSCC. Using reverse phase protein array (RPPA), we conducted an integrative proteomic-genomic analysis on HNSCC patient tumors. We sought to determine whether *PTPR* mutation is correlated with altered STAT3(Y705) phosphorylation in primary HNSCC tumor specimens. Strikingly, examination of 212 HNSCC primary tumors showed that tumors harboring mutations in *PTPR* tumor suppressor genes (including *PTPRD/J/K/M/O/S/T*) (3) expressed significantly higher levels of p-STAT3(Y705) compared with tumors with wild-type *PTPR* family members ($P = 0.02$) (Fig. 1*A*). These results provide evidence of a direct association between *PTPR* mutation and elevated STAT3 phosphorylation/activation in human tumors in situ and establish a plausible mechanism for STAT3 hyperactivation in human cancers. In contrast, we observed no correlation between p-STAT3(Y705) expression and epidermal growth factor receptor (EGFR), p-EGFR(Y1068), p-EGFR(Y1173), suppressor of cytokine signaling (SOCS), Src, or interleukin 6 (IL6) expression. Additionally, HNSCC tumors harboring multiple *PTPR* mutations exhibited an even greater increase in p-STAT3(Y705) expression although the number of tumors in these groups is insufficient for statistical analysis (n = 14, 2, 1, or 1, for tumors with 2, 3, 4, or 5 *PTPR* mutations per tumor, respectively). Upregulation of p-STAT3(Y705) was further confirmed by immunohistochemistry in HNSCC tumors harboring PTPR mutations (Fig. S1) and in HNSCC cell lines harboring endogenous PTPR mutations (Fig. S2).

PTPRT Mutations "Drive" HNSCC Cell Survival and STAT3 Activation. The biologic/functional consequences of tumor-derived *PTPR* mutations in HNSCC are unknown. To determine whether HNSCC *PTPRT* mutations act as "drivers," we developed a serum-dependent HNSCC cell line (PCI-52-SD1) that undergoes rapid cell death in the absence of serum. Using this model, stable expression of two representative mutants (calculated to result in

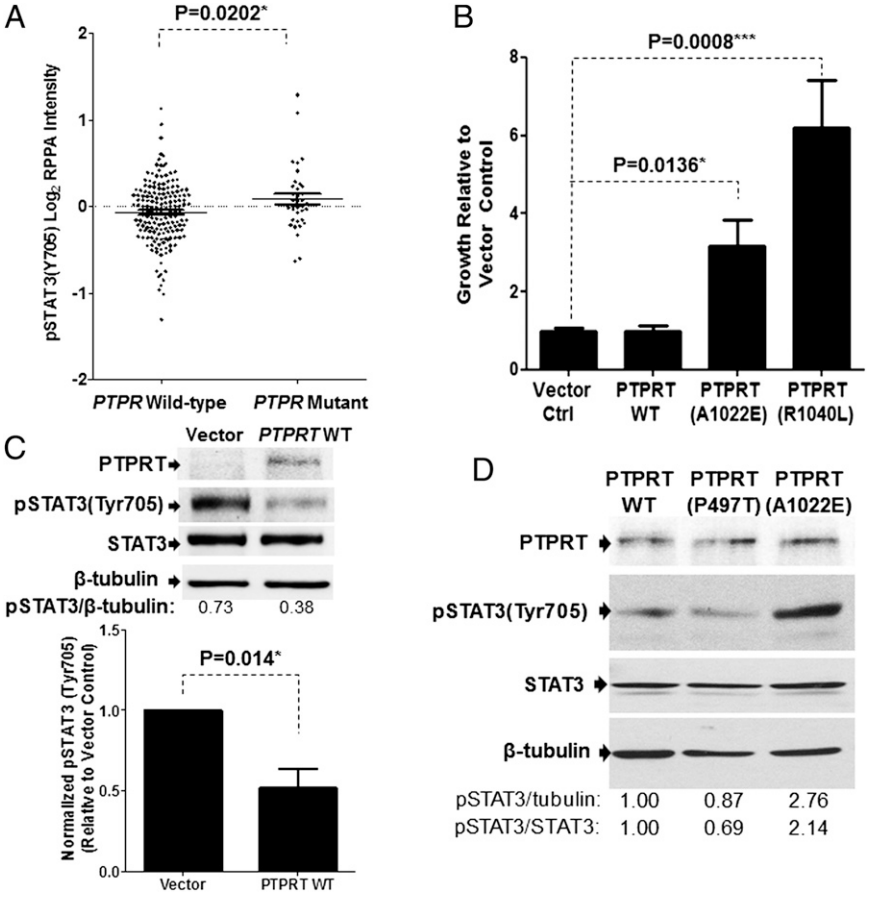

Fig. 1. PTPR mutations correlate with STAT3 tyrosine phosphorylation in HNSCC tumors and enhance survival and STAT3 phosphorylation in HNSCC cells. (*A*) Significant increase in p-STAT3(Y705) expression (intensity plot in $\log_2$ scale; protein array data from The Cancer Proteome Atlas) in HNSCC patient tumors harboring PTPRD/J/K/M/O/S/T mutation (n = 37) vs. tumors without PTPRT mutation (n = 171) ($P = 0.0202$*). (*B*) Serum-dependent PCI-52-SD1 cells stably expressing EGFP-vector control, wild-type PTPRT, or PTPRT(A1022E) or (R1040L) mutants were assessed by MTT assay for growth in the absence of serum. Cumulative growth relative to vector control ($n \geq 9$) is shown. (*C*) Stable expression of wild-type PTPRT reduced basal p-STAT3(Tyr705) expression in PCI-52-SD1 cells. Graph showing cumulative results of p-STAT(Y705) levels in these cells from five independent experiments. (*D*) CAL-33 cells were transiently transfected with a representative PTPase-domain mutation (A1022E) and an FN3-domain mutation (P497T). Expression levels of p-STAT3 (Tyr705) were detected by Western blotting. The PTPase domain mutation, but not the FN3-domain mutation, increased p-STAT3(Tyr705) expression. Similar results were observed in three independent experiments.

both charge and amino acid size changes) (Table S1), PTPRT (A1022E) and PTPRT(R1040L), conferred increased survival (3.2- and 6.2-fold, respectively) compared with expression of empty vector control, confirming a driver phenotype for these *PTPRT* mutants in HNSCC cells (Fig. 1*B*).

To investigate the mechanism responsible for the driver phenotype of the *PTPRT* mutants, we tested the hypothesis that *PTPRT* mutations identified in HNSCC may impair the phosphatase activity of the enzyme, resulting in increased phosphorylation of PTPRT substrates, including the oncogenic transcription factor STAT3. Stable expression of wild-type PTPRT in PCI-52-SD1 cells resulted in reduction of basal p-STAT3 levels by ~48% ($P = 0.0014$) (Fig. 1*C*), demonstrating that wild-type PTPRT can modulate STAT3 activation in HNSCC cells. On the other hand, expression of a PTPRT protein harboring a mutation (A1022E) in the catalytic domain promoted up-regulation of the p-STAT3 protein in an HNSCC cell line with low basal levels of p-STAT3 (CAL-33) (Fig. 1*D*). Similar effects were observed in HEK293 cells upon transient expression of a PTPRT mutant (Fig. S3). Interestingly, expression of a PTPRT protein with a mutation (P497T) in the extracellular fibronectin type III-like domain did not alter the phosphorylation status of STAT3 (Fig. 1*D*), suggesting that mutations outside the catalytic domains may have other mechanisms of action. In addition, expression of wild-type PTPRT in EGFR-knockout mouse embryonic fibroblasts resulted in decreased expression of p-STAT3 (Y705), suggesting that PTPRT catalytic activity is independent of EGFR expression/activity (Fig. S4).

Computational Modeling of PTPRT Mutations in the Substrate Binding Sites Reveals Plausible Functional Alterations of Phosphatase Activity. Given that a high percentage of PTPRT mutations are located within the enzymatic (PTPase) domain, we sought to determine the potential impact of these mutations on interactions between the catalytic domains and phospho-tyrosine substrate using a molecular modeling approach. Although the structure of a PTPRT–p-Tyr protein complex is not available, the X-ray crystallographic structure of the PTPRT phosphatase domain alone has been reported (PDB ID code 2OOQ) (8). Therefore, we determined by homology modeling (9), the approximate substrate-interacting surface of the PTPRT PTPase domains 1 and 2 (Fig. 2 *A*–*D*) based on the highly similar (to PTPRT) crystal structure of human tyrosine phosphatase PTPN5 in complex with p-Tyr (detailed in *Materials and Methods*). Using this model, we localized several cancer-related *PTPRT* mutation sites to the substrate-interaction surface of the PTPRT PTPase domains 1 and 2 in close proximity to incorporated p-Tyr (D905, R928, H1053, G1089, and V1124 in domain 1; Q1180, R1201, R1207, P1213, Q1286, T1346, N1380, G1382, and R1384 in domain 2). Mutation sites previously shown to decrease the PTPRT phosphatase activity were also found in proximity to p-Tyr regions (C1084, D1052, Y893, Q965, R1188, and T1346) (10, 11). These results suggest that PTPRT PTPase domain mutations, which are found in human cancers, likely interfere with enzymatic activity and/or substrate interactions. Of note, in addition to the reported missense mutations of the PTPRT PTPase domains, many nonsense mutations (mutation to a stop codon) and frameshift mutations are highly likely to alter PTPRT structure and stability, as well as impacting substrate interactions (L362fs, R617fs, Q434*, and Q615* found in HNSCC, and E1227*, R1207*, E1155*, R1358*, and G1386* in other cancers; COSMIC database).

PTPR Genes Are Mutated in Nearly One-Third of HNSCC Tumors, and PTPRT Is the Most Frequently Mutated PTPR. *PTPRT* belongs to the receptor protein tyrosine phosphatase family, which comprises 21 members, and no genomic study to date has examined the mutational profile of the entire family in a large number of human tumor specimens. To understand the potential genetic contributions of the *PTPR* family (in addition to *PTPRT*) to tyrosine signaling/regulation in head and neck squamous cell carcinoma (HNSCC), we comprehensively analyzed *PTPR* family mutations in large cohorts of primary HNSCC tumors. Whole-exome sequencing data of 374 primary HNSCCs were included [from 300 TCGA HNSCC tumors and 74 HNSCCs previously published (12)]. Strikingly, 30.7% (115/374) of HNSCC tumors harbored nonsynonymous somatic mutations of at least one *PTPR* family member, compared with only 15.2% (57/374) of tumors with mutations of cytoplasmic PTP genes, the second major family of PTPs (Fig. 3*A*). Further, 7.8% (29/374) of HNSCC tumors contained multiple mutations of *PTPR* family members (from two to six *PTPR* mutations/tumor) (Fig. 3*B*) (Table S2 contains all *PTPR* mutations found in HNSCC). Further investigation demonstrated that this high rate of somatic mutation of the *PTPR* family (vs. cytoplasmic PTPs) found in HNSCC is also detected in all 14 types of human solid tumors sequenced to date by The Cancer Genome Atlas (TCGA) (4,039 total solid tumors sequenced), but not in a hematopoietic malignancy (6/196 AML cases; 3.1%) (Fig. 3*C* and Table S3), implicating a likely pathologic involvement of *PTPR* mutations in HNSCC, as well as other solid human tumors.

Human papilloma virus (HPV) infection is a known etiologic factor in a subset of HNSCC and is capable of disrupting genome stability. Thus, we examined whether HPV was associated with the high rate of *PTPR* mutations in HNSCC. Statistical analysis showed no correlation between *PTPR* mutation and HPV status ($P = 0.31$; *PTPR* mutations in 11/48 HPV-positive tumors vs. 93/299 HPV-negative tumors), indicating that HPV is not a contributing factor to *PTPR* mutations in HNSCC. Further analysis showed that *PTPR* mutations were not associated with mutations of *TP53* ($P = 0.81$), *NOTCH1* ($P = 0.24$), *PIK3CA* ($P = 0.47$), or *HRAS* ($P = 0.77$) in HNSCC, indicating that *PTPR* mutations are independent of these known common mutational events in HNSCC tumors (12).

The availability of comprehensive whole-exome sequencing data (from TCGA) on all *PTPR* genes allowed us to identify the most commonly mutated *PTPRs* in all sequenced human cancers, including HNSCC. Among the 374 sequenced HNSCC tumors, *PTPRT* is the most frequently mutated *PTPR* (5.6% cases; 22 mutations total, with one tumor harboring 2 *PTPRT* mutations), followed by *PTPRC*, *PTPRD*, and *PTPRM* (Table S2). Although *PTPR* mutation rates vary among different cancer types, cumulative results reveal that *PTPRT* is the single most commonly mutated *PTPR* in human cancers (6.2%, 285 mutations in 4,609 solid and hematopoietic cancers sequenced) (Table S3), with the highest mutation frequency of *PTPRT* in cutaneous melanoma (a total of 99 mutations in 253 tumors sequenced; 39.1%).

The sites of the most frequently mutated *PTPR* members (*PTPRT*/*C*/*D*/*M*) in HNSCC are shown in Fig. 3*D* (all other HNSCC-associated *PTPR* mutations are shown in Fig. S5). Cumulative mutation data for *PTPRT* in 16 types of sequenced tumors indicate that 37.9% (108/285) of *PTPRT* mutations are found in the catalytic phosphatase (PTPase) domain whereas 33.0% (94/285) occur in the extracellular fibronectin type III-like (FN3) domain. In HNSCC, 45.5% (10/22) of *PTPRT* mutations are located in the PTPase domain (Fig. 3*D*), indicating the pathologic relevance of these genetic alterations of the phosphatase activity, which lead to pSTAT3 up-regulation in HNSCC tumors.

Discussion

These cumulative results indicate that selected tumor-associated *PTPRT* mutations can alter STAT3 phosphorylation/activation. Our findings suggest a previously undescribed, and potentially common, mechanism for dysregulated cell survival and growth involving *PTPR* mutation and STAT3 hyperactivation. Therefore, tumors that harbor *PTPR* (including *PTPRT*) mutations may be amenable to treatment with STAT3 pathway inhibitors. The frequency of *PTPR* mutations is unexpectedly high across all solid tumor types analyzed to date. The dispersed distribution and lack of hotspot mutations in *PTPR* genes suggest that these mutations likely represent loss-of-function events affecting tumor suppressive proteins rather than gain-of-function of oncogenic proteins in cancer. Although this mutation pattern is consistent with that reported for select *PTPRs* in colorectal cancers (10), this study represents a comprehensive analysis of somatic mutations of the entire *PTPR* family across all human cancers sequenced to date.

Constitutive STAT3 activation is frequently found in nearly all human cancers, and expression levels of p-STAT3(Y705)

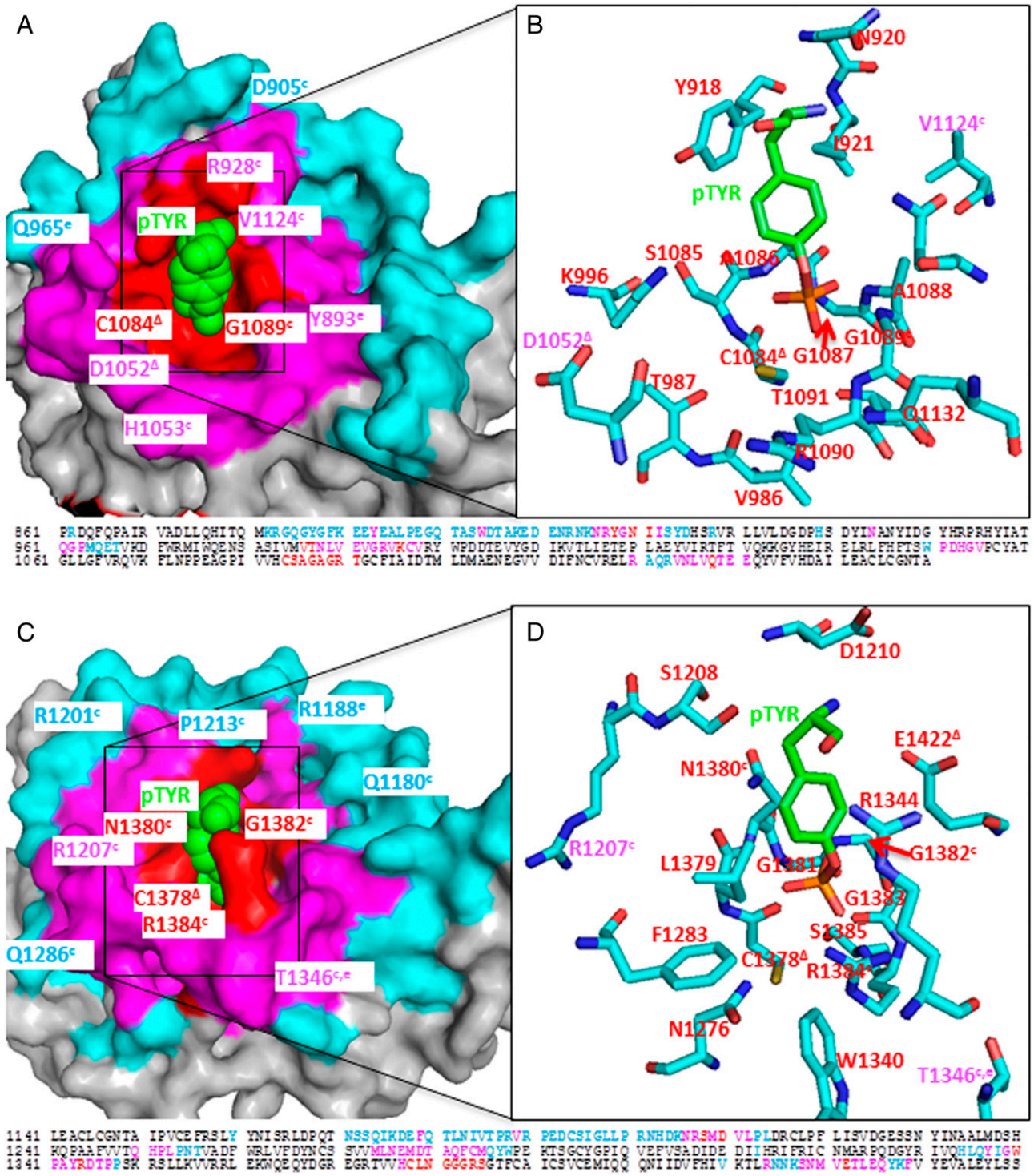

Fig. 2. Computational modeling of PTPRT PTPase domain in complex with a phospho-tyrosine substrate. (*A*) PTPRT PTPase domain 1 in complex with phospho-tyrosine (p-Tyr, green) of substrate (e.g., p-STAT3). The surface involved in the interaction with partner (p-Tyr-containing) protein is divided into three regions, residues within 0–5 Å from p-Tyr (red), 5–12 Å (purple), and 12–25 Å (cyan). Positions found to be mutated in human cancers are indicated by "c"; trapping mutations by "Δ" (6); other experimentally verified loss-of-function mutations by "e" (10, 11). (*B*) Detailed view of the catalytic site. The largest part of the catalytic site in domain 1 is formed by the loop region (from the catalytic C1084-G1092). Positively charged R1090 and K996 are involved in the electrostatic interaction with the negatively charged phosphate group of p-Tyr. The aromatic part of p-Tyr is further stabilized by hydrophobic interactions with Y918 and I921. (*C*) Structure of the PTPRT PTPase domain 2 in complex with p-Tyr (green) of the binding partner (e.g., p-STAT3). Annotations are as in *B*. Potential trapping mutations based on homology with domain 1 are indicated by "Δ". (*D*) Detailed view of the catalytic site of the PTPRT PTPase domain 2.

are often associated with poor prognosis (13–15). Mechanisms driving STAT3 activation in cancer are incompletely understood. Direct sequencing of thousands of patient tumors by TCGA has not identified common or consistent STAT3 mutational events in solid tumors. Furthermore, solid tumors, including HNSCC, exhibit a lack of activating mutations in kinases upstream

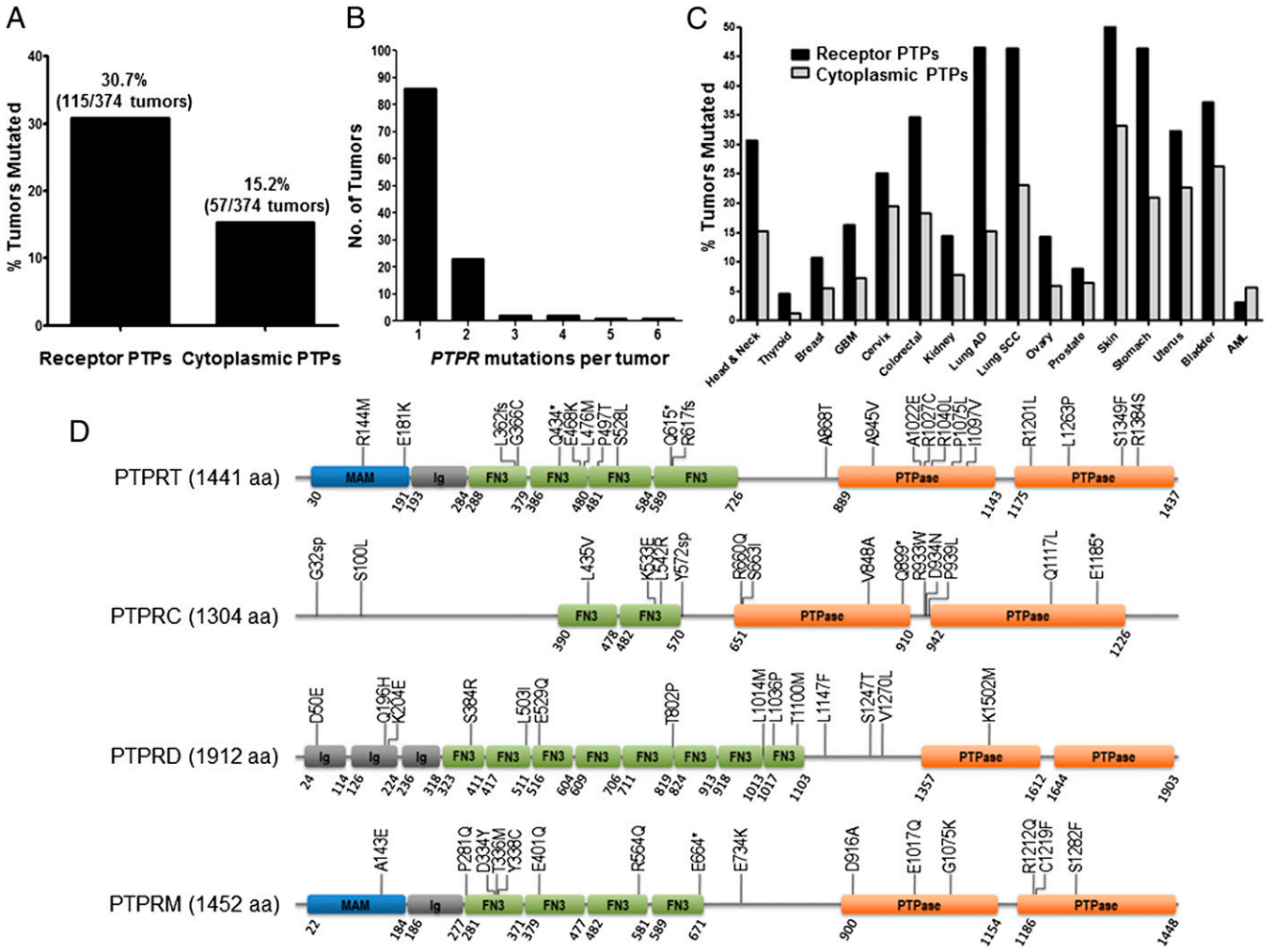

Fig. 3. Whole-exome sequencing of human cancers demonstrates high rates of PTPR somatic mutations. (*A*) Frequencies of *PTPR* (the receptor subtype) and cytoplasmic PTP somatic mutations in 374 HNSCC tumors. (*B*) A subset (29/374, 7.8%) of HNSCC tumors harbor mutations of multiple *PTPR* genes. (*C*) The *PTPR* gene family is mutated at a higher rate than the cytoplasmic PTP gene family across 15 cancers [cBio portal (24)]. AD, adenocarcinoma; AML, acute myeloid leukemia; GBM, glioblastoma multiforme; SCC, squamous cell carcinoma. (*D*) Mutation and domain-mapping of the four most frequently mutated RPTPs in HNSCC. Domains defined as in the Swiss-Prot entries, Protein Knowledgebase, and UniProtKB.

of STAT3 (4). Thus, activating mutations of STAT3, or of direct upstream positive regulators, are unlikely to be the key genetic factors driving STAT3 hyperactivation in human cancers. PTPRT has been reported to be a negative regulator of STAT3 (6). Our integrative genomic-proteomic findings establish that *PTPRT* mutations are important genetic events that drive in situ up-regulation of p-STAT3(Y705) within patient tumors. This reveals the driver role of genetic mutations in a negative regulator(s) of STAT3, an important oncogenic signaling protein in human cancer. PTPRT has been previously shown to be a tumor suppressor (in colon cancer cell line models), consistent with our present findings (16). Our results suggest that loss-of-function mutations in tumor suppressor tyrosine phosphatases may not only serve as permissive factors for oncogenesis as previously demonstrated, but can also act as direct drivers for cancer cell growth via dysregulation of substrate tyrosine phosphorylation.

Studies of PTPRT, in particular, showed that PTPRT has a discretely defined set of substrates, including STAT3 and paxillin. In our current study, the correlation between paxillin phosphorylation and *PTPRT* mutations was not examined, as anti–phospho-paxillin antibody has not been validated for our protein array platform. However, it is possible that paxillin signaling may also be affected by *PTPRT* mutations in the human tumors.

Computational modeling allows us to predict the potential effects of PTPase domain mutations (located intracellularly) in PTPRT, which may be applicable to other RPTP proteins. However, there are no existing computational methodologies to reliably predict the effects of the extracellular domain mutations (such as the FN3 domain mutations) found in these proteins. The broad existence of these extracellular domain mutations in the RPTP family will require systematic functional validation of each mutation in relevant cell models, as we have previously shown that some of these mutations could alter cell–cell adhesion, and thereby promote tumor cell migration (17).

The present study demonstrates that wild-type PTPRT promotes down-regulation of p-STAT3(Y705) in HNSCC and that somatic *PTPRT* mutations may represent "driving" events in cancer. We identify that somatic *PTPR* mutations, including *PTPRT* mutations, are associated with elevated p-STAT3(Y705) in human HNSCC. Other RPTP family members, especially *PTPRD,* may play similar roles in HNSCC and other solid tumors, where somatic mutation may lead to loss-of-function and subsequent activation of oncogenic pathways. Indeed, several commonly mutated *PTPR*s have been implicated as tumor suppressors, including *PTPRD* (18), *PTPRF* (10), *PTPRG* (10, 19), *PTPRJ* (20), and *PTPRS* (21).

In conclusion, *PTPR* mutational events are relatively common in primary HNSCC, as well as in many other solid tumors as revealed by large-scale whole-exome sequencing studies. We demonstrate that tumor-specific mutational events in the *PTPRT* gene can serve as direct drivers for tumor growth by inducing hyperactivation of STAT3, a potent oncogenic transcription factor and PTPRT substrate. STAT3 pathway inhibitors are under active investigation in human cancers and include transcription factor decoys, disruptors of recruitment of STAT3 to the IL6/IL6Ralpha/gp130 complex, and upstream kinase inhibitors, primarily Janus kinase inhibitors (22, 23). It is biologically plausible that selected *PTPR* mutations may identify tumors that may be particularly responsive to treatment with STAT3 pathway inhibitors.

Materials and Methods

Mutation Databases. HNSCC mutation analyses were based on the published whole-exome sequencing data on 74 HNSCC tumors (12) and TCGA. *PTPR* and cytoplasmic PTP family mutation rates (% mutated tumors) were calculated by the actual percent of tumors harboring nonsynonymous mutations of *PTPR* or cytoplasmic PTP family members. For multicancer analysis, mutation data (from whole-exome sequencing) were obtained from the cBio portal (24).

Proteomic Analysis. Quantitative proteomic analysis (reverse phase protein array) of p-STAT3(Y705) was performed on 212 HNSCC tumors (a subset of the 374 tumors in this study). Data were obtained from The Cancer Proteome Atlas (TCPA) database (http://app1.bioinformatics.mdanderson.org/tcpa/_design/basic/index.html). Phospho-STAT3(Y705) expression levels of the *PTPR*-WT versus *PTPR*-mutated tumors were compared using a two-tailed *t* test in GraphPad Prism 5 software (GraphPad).

Cell Cultures. All HNSCC cell lines were genotypically verified and grown in a humidified cell incubator at 37 °C and 5% (vol/vol) CO_2. CAL-33, Cal27, FaDu, and PCI-52 cells were maintained in complete DMEM containing 10% FBS and 1× penicillin/streptomycin solution (Invitrogen) whereas PE/CA-PJ34.12 and PE/CA-PJ49 cells were maintained in IDMEM containing 10% (vol/vol) FBS and 2 mM L-glutamine. Cal27 and FaDu cell lines were obtained from ATCC whereas PE/CA-PJ34.12 and PE/CA-PJ49 cells were obtained from Sigma-Aldrich. CAL-33 cells were obtained from Gerard Milano (Centre Antoine Lacassagne, Nice, France), and the PCI-52-SD1 cell line was obtained by clonal selection of the parental PCI-52 cell line (University of Pittsburgh Cancer Institute) by rounds of graded serum selection. In brief, PCI-52 parental cell lines were plated as single cells, which grew as single clones. These single clones were subjected to serum deprivation (0% FBS) for 1–2 wk, followed by assessment of cell growth by 3-[4,5-dimethylthiazol-2-yl]-2,5 diphenyl tetrazolium bromide (MTT) assay. The PCI-52-SD1 subline was the most serum-sensitive subline, which died (>99.8%) upon complete serum deprivation.

Plasmid Constructs and Site-Directed Mutagenesis. pCI-Neo-PTPRT was obtained from Addgene (plasmid 16630). pMXs-puro-EGFP vector was obtained from Cell Biolabs. *PTPRT* WT gene was subcloned into the retroviral vector, and the pMXs-puro-*PTPRT* WT was used as a template for site-directed mutagenesis using the QuikChange Site-Directed Mutagenesis Kit according to the manufacturer's instructions (Stratagene). All mutation sites as well as the full-length cDNA were sequence confirmed.

Retroviral Infection of HNSCC Cells. Retroviruses were generated using the Platinum Retrovirus Expression Systems (Cell Biolabs) according to the manufacturer's instructions. Briefly, Plat-A cells were transfected with 3 μg of retroviral vector carrying the gene of interest (pMXs-puro-*EGFP* as control, pMXs-puro-*PTPRT* WT, pMXs-puro-*PTPRT* mutants). Three days after transfection, fresh retroviruses (in the supernatant of the Plat-A cells) were collected by centrifugation at 1,200 × *g* for 5 min at 4 °C. Cell debris was removed by filtering through a 0.45-μm syringe filter. Fresh retroviruses were used for infection of HNSCC cells. HNSCC cells were plated at 20% confluency in a T75 flask 1 d before infection. Infection of HNSCC cells was performed by adding 4.5 mL of retrovirus to the cells containing 7.5 mL of complete culture media. Then, 38 μL of polybrene (4 μg/μL; Sigma-Aldrich) was added to the cells with gentle mixing. Cells were then incubated at 37 °C and 5% CO_2 for an additional 48–72 h, and the infection medium was replaced with fresh complete medium. Expression of the gene of interest and alteration of the signaling pathway were assessed within 7–10 d of infection.

Immunoblotting. Primary antibodies for p-STAT3(Tyr705) and STAT3 were purchased from Cell Signaling Technology. PTPRT antibody was produced by Z.W. Anti-tubulin antibody was from Abcam, and secondary antibodies were from BioRad. Blots were quantitated by densitometry using ImageJ software.

Molecular Modeling. The crystal structure of human PTPRT catalytic domain 1 (PDB ID code 2OOQ) (8) and the crystal structure of catalytic domains 1 and 2 of human protein phosphatase gamma (PDB ID code 2NLK) (8) were used as templates for homology modeling of human PTPRT (amino acids 862–1441, covering the PTPase domains 1 and 2) using the program Modeler version 9v8 (9). A substrate, p-Tyr, was modeled into the catalytic sites of both domains 1 and 2 of PTPRT upon superposition with the highly similar crystal structure of the human tyrosine phosphatase PTPN5 (also known as STEP) (C472S catalytically inactive mutant) in complex with p-Tyr (PDB ID code 2CJZ) (the root-mean-square deviation between 2OOQ and 2CJZ is 1.85 Å). Surface residues of the PTPRT PTPase domain 1 and 2 were divided into three groups according to their distance from the bound p-Tyr (within 0–5 Å, 5–12 Å, and 12–25 Å).

ACKNOWLEDGMENTS. This work was supported by National Institutes of Health Grants P50CA097190 and R01CA77308 and the American Cancer Society (to J.R.G.), the Patricia L. Knebel Fund of the Pittsburgh Foundation (V.W.Y.L.), National Institutes of Health Grants R01 CA137260 (to D.E.J.), R01 CA127590 (to Z.W.), and F31 DE024007, and a Department of Pharmacology and Chemical Biology, University of Pittsburgh School of Medicine, John S. Lazo Cancer Pharmacology Fellowship (to N.D.P.). Support for training and career development of researchers (Marie Curie) came from an International Outgoing Fellowship of the European Community program, Contracts PIOF-GA-2009-235902 (to J.H.) and P41 GM103712 (to I.B.).

1. Groesser L, et al. (2012) Postzygotic HRAS and KRAS mutations cause nevus sebaceous and Schimmelpenning syndrome. *Nat Genet* 44(7):783–787.
2. Paez JG, et al. (2004) EGFR mutations in lung cancer: Correlation with clinical response to gefitinib therapy. *Science* 304(5676):1497–1500.
3. Julien SG, Dubé N, Hardy S, Tremblay ML (2011) Inside the human cancer tyrosine phosphatome. *Nat Rev Cancer* 11(1):35–49.
4. Lui VW, et al. (2013) Frequent mutation of the PI3K pathway in head and neck cancer defines predictive biomarkers. *Cancer Discov* 3(7):761–769.
5. Gao SP, et al. (2007) Mutations in the EGFR kinase domain mediate STAT3 activation via IL-6 production in human lung adenocarcinomas. *J Clin Invest* 117(12):3846–3856.
6. Zhang X, et al. (2007) Identification of STAT3 as a substrate of receptor protein tyrosine phosphatase T. *Proc Natl Acad Sci USA* 104(10):4060–4064.
7. Veeriah S, et al. (2009) The tyrosine phosphatase PTPRD is a tumor suppressor that is frequently inactivated and mutated in glioblastoma and other human cancers. *Proc Natl Acad Sci USA* 106(23):9435–9440.
8. Barr AJ, et al. (2009) Large-scale structural analysis of the classical human protein tyrosine phosphatome. *Cell* 136(2):352–363.
9. Sali A, Blundell TL (1993) Comparative protein modelling by satisfaction of spatial restraints. *J Mol Biol* 234(3):779–815.
10. Wang Z, et al. (2004) Mutational analysis of the tyrosine phosphatome in colorectal cancers. *Science* 304(5674):1164–1166.
11. Lim SH, et al. (2009) Synapse formation regulated by protein tyrosine phosphatase receptor T through interaction with cell adhesion molecules and Fyn. *EMBO J* 28(22):3564–3578.
12. Stransky N, et al. (2011) The mutational landscape of head and neck squamous cell carcinoma. *Science* 333(6046):1157–1160.
13. Chen Y, et al. (2013) STAT3, a poor survival predicator, is associated with lymph node metastasis from breast cancer. *J Breast Cancer* 16(1):40–49.
14. Macha MA, et al. (2011) Prognostic significance of nuclear pSTAT3 in oral cancer. *Head Neck* 33(4):482–489.
15. Kusaba T, et al. (2006) Activation of STAT3 is a marker of poor prognosis in human colorectal cancer. *Oncol Rep* 15(6):1445–1451.
16. Scott A, Wang Z (2011) Tumour suppressor function of protein tyrosine phosphatase receptor-T. *Biosci Rep* 31(5):303–307.
17. Yu J, et al. (2008) Tumor-derived extracellular mutations of PTPRT /PTPrho are defective in cell adhesion. *Mol Cancer Res* 6(7):1106–1113.
18. Solomon DA, et al. (2008) Mutational inactivation of PTPRD in glioblastoma multiforme and malignant melanoma. *Cancer Res* 68(24):10300–10306.
19. Cheung AK, et al. (2008) Functional analysis of a cell cycle-associated, tumor-suppressive gene, protein tyrosine phosphatase receptor type G, in nasopharyngeal carcinoma. *Cancer Res* 68(19):8137–8145.
20. Ruivenkamp CA, et al. (2002) Ptprj is a candidate for the mouse colon-cancer susceptibility locus Scc1 and is frequently deleted in human cancers. *Nat Genet* 31(3):295–300.
21. Korff S, et al. (2008) Frameshift mutations in coding repeats of protein tyrosine phosphatase genes in colorectal tumors with microsatellite instability. *BMC Cancer* 8:329.
22. Dymock BW, See CS (2013) Inhibitors of JAK2 and JAK3: An update on the patent literature 2010 - 2012. *Expert Opin Ther Pat* 23(4):449–501.
23. Nallar SC, et al. (2013) Tumor-derived mutations in the gene associated with retinoid interferon-induced mortality (GRIM-19) disrupt its anti-signal transducer and activator of transcription 3 (STAT3) activity and promote oncogenesis. *J Biol Chem* 288(11):7930–7941.
24. Cerami E, et al. (2012) The cBio cancer genomics portal: An open platform for exploring multidimensional cancer genomics data. *Cancer Discov* 2(5):401–404.